# THE EFFECT OF WIND TUNNEL CONSTRAINT ON UNSTEADY AERODYNAMICS EXPERIMENTS

by

R.B. Green and R.A.McD. Galbraith,
Department of Aerospace Engineering,
University of Glasgow,
Glasgow,
Scotland.
G12 8QQ

**Abstract**

The effects of wind tunnel constraint during low speed unsteady aerodynamics experiments are assessed by comparing the data from two NACA 0015 models, one with a chord length of half the other. To distinguish between the effects of constraint upon separation and attachment, ramp-up and ramp-down tests are considered. It emerges that the unsteady separation process measured in terms of the normal force, pitching moment and stall vortex convection speed is virtually unaffected by the difference in constraint between the two models, while the attachment process, assessed in terms of the normal force response and attachment behaviour, is sensitive to the size of the model.

**Nomenclature**

| | |
|---|---|
| AR | aspect ratio |
| c | aerfoil chord (m) |
| $C_n$ | normal force coefficient |
| $C_m$ | quarter chord pitching moment coefficient |
| DP | dynamic pressure |
| R | $Re/10^6$ |
| r | reduced pitch rate ($\dot{\alpha}\pi c/360U$) |
| Re | Reynolds number |
| t | time (s) |
| U | free stream speed ($ms^{-1}$) |
| u | stall vortex convection speed ($ms^{-1}$) |
| x | distance along chord (m) |
| $\alpha$ | incidence (deg) |
| $\dot{\alpha}$ | linear pitch rate (deg $s^{-1}$) |

## 1. Introduction

The field of unsteady aerodynamics has been intensively studied over the years, as its effects must be considered in the design of helicopter rotors, highly manouevrable aircraft, fluttering compressor blades and wind turbines. In the severest circumstances the effects of unsteady separation, vortex formation and convection and unsteady reattachment must be considered, and these phenomena are also of importance from a fundamental point of view. However, in spite of the considerable effort expended in investigating unsteady aerodynamics, the effects of wind tunnel constraint during experimental tests are virtually unknown, and this is the subject of the present paper.

Dynamic stall occurs when an aerofoil is pitched to well above the normal static stall incidence, and is characterised by the formation and convection over the upper surface of the aerofoil of a powerful, well organised vortex; the stall vortex [1]. From the results of tests carried out on seven aerofoil models at the University of Glasgow, Green et al. [2] showed that the stall vortex convection speed was independent of aerofoil motion to a first order. However, the results of other data sets show that this is not the case, the result of Lorber & Carta [3] in particular showing a linear convection speed/ reduced pitch rate dependency. Although the aerofoil model may be important (Green et al.[4]), it was felt that the effect of wind tunnel constraint needed consideration.

While unsteady aerodynamics experiments have mainly focussed upon dynamic stall, little attention has been paid to the process of unsteady attachment from the separated state. The phenomenon of negative lift at positive incidence during ramp-down motion from the separated state has been observed at the University of Glasgow by Niven et al.[5] for a variety of aerofoils. It was postulated that this phenomenon was due to different response rates of the attached flow on the lower surface and the separated flow on the upper surface to the aerofoil motion. Since this phenomenon had not been reported elsewhere, they conceded that it may in fact be a three dimensional effect, especially since flow visualisation showed that the separated flow at high incidence during a static test was highly three-dimensional. Further analysis by Niven and

Galbraith [6] showed that downwash in the wind tunnel could not reasonably account for the negative lift at positive incidence, while ramp-down tests from different start incidences and the presence of splitter plates (which therefore affect the degree of three-dimensionality of the starting separated flow) did not affect the overall result.

The problems discussed above obviated the need to build and test, using the same wind tunnel facility, an aerofoil model of half the chord length of the models previously tested at the University of Glasgow. The alternative to testing the new model would be to correct for wind tunnel constraint effects. No adequate unsteady correction techniques are available, however, so as well as contributing to assessing the above anomalies, a general appreciation of constraint effects upon unsteady aerodynamics experiments would be gained.

Described in this paper are a series of comparisons of data between the results of two NACA 0015 models tested using the unsteady aerodynamics facility at the University of Glasgow[4]. Dynamic stall results during ramp-up motions of the two models are compared in terms of the stall onset, peak $C_n$ and $C_m$ and stall vortex convection speed. Unsteady attachment results are compared in terms of the $C_n$ and attachment behaviour during ramp-down motions.

## 2. The University of Glasgow Unsteady Aerodynamics Test Facility

The general arrangement of the model in the wind tunnel is illustrated in figure 1.

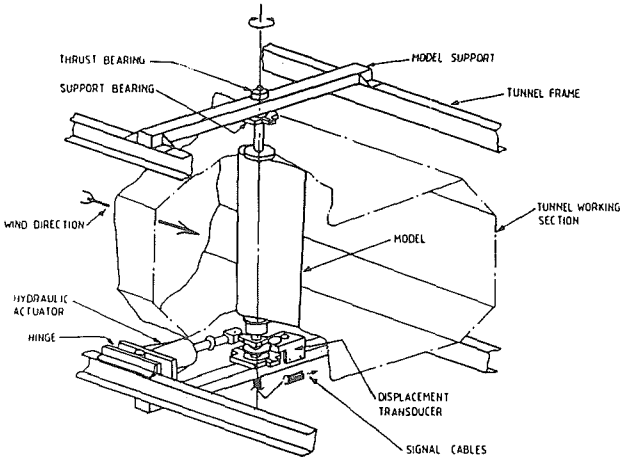


Figure 1 The University of Glasgow Handley-Page wind tunnel and unsteady aerodynamics facility

The large chord NACA 0015 (hereafter referred to as model 5) had a chord length of 0.55m and a span of 1.61m, and was constructed of a fibre glass skin filled with an epoxy resin foam and bonded to an aluminium spar. The small chord NACA 0015 (referred to as model 12) was identical to model 5 except that the chord length was 0.275m and the spar was made of steel. Each model was mounted vertically in the University of Glasgow's Handley-Page wind tunnel, which is a closed return type with a 1.61mx2.13m octagonal working section. Thus model 5 had a blockage coefficient and aspect ratio of 0.26 and 2.92, while the respective figures for model 12 were 0.13 and 5.84.

The aerofoil was pivoted about the quarter chord using a linear hydraulic actuator and crank mechanism. Instantaneous aerofoil incidence was measured using a linear angular potentiometer geared to the model's tubular support. The dynamic pressure in the working section was obtained from the difference between the static pressure in the working section, about 1.2m upstream of the leading edge, and the static pressure in the settling chamber, as measured by an electronic micromanometer. Thirty ultra-miniature pressure transducers (type KULITE XCS-093-PSI G) were installed below the surface of the centre span of each model, and their locations are shown in figure 2.

| UPPER SURFACE | | LOWER SURFACE | |
|---|---|---|---|
| channel | x/c | channel | x/c |
| 1 | 0.98 | 16 | 0.0003 |
| 2 | 0.95 | 17 | 0.0025 |
| 3 | 0.83 | 18 | 0.01 |
| 4 | 0.70 | 19 | 0.025 |
| 5 | 0.59 | 20 | 0.05 |
| 6 | 0.50 | 21 | 0.10 |
| 7 | 0.37 | 22 | 0.17 |
| 8 | 0.26 | 23 | 0.26 |
| 9 | 0.17 | 24 | 0.37 |
| 10 | 0.10 | 25 | 0.50 |
| 11 | 0.05 | 26 | 0.59 |
| 12 | 0.025 | 27 | 0.70 |
| 13 | 0.01 | 28 | 0.83 |
| 14 | 0.0025 | 29 | 0.95 |
| 15 | 0.0003 | 30 | 0.98 |

Figure 2 Aerofoil profile and transducer positions for the NACA 0015 models

After signal conditioning, the outputs of the pressure transducers were passed to a sample-and-hold module. For the model 5, data logging was performed using a DEC MINC, while for the model 12 a Thorn EMI BE256 controlled by an IBM model 80 was used. Five data sweeps containing 256 data samples were recorded at up to 550Hz per channel using the MINC based system, while 6 data sweeps containing 1024 data samples recorded at up to 50KHz per channel were available from the IBM/BE256 system. After sampling the data were reduced, averaged and stored on a DEC MicroVAX for subsequent analysis.

## 3. Results

The following sections present a comparison of data between the model 5 and the model 12 for static tests, ramp-up and ramp-down motions. Unfortunately the wind tunnel was not available for a full series of tests on model 5 at R=1.0, so therefore most of the comparisons will be between the model 12 at R=1.0 and the model 5 at R=1.5. Re effects will be considered, however, before an assessment of constraint effects is made.

### 3.1 Static tests

A comparison of the static test data between the two models can reveal much about possible differences in stall type; figure 3 shows such a comparison at R=1.07.

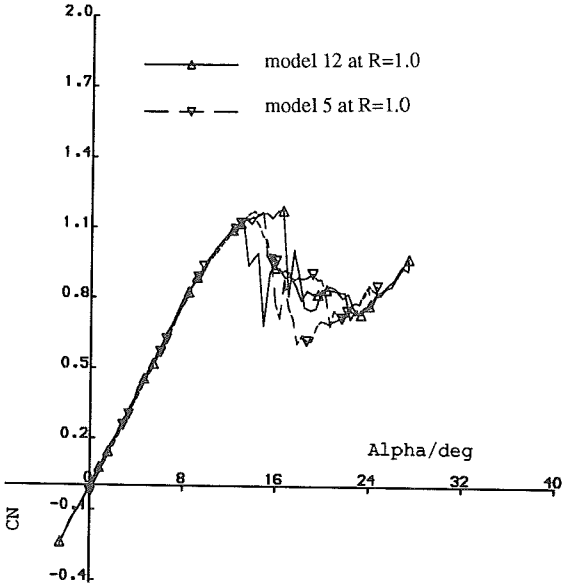


Figure 3 $C_n$ plotted against $\alpha$. Static test for model 12 and model 5 at R=1.0

The agreement of the two curves prior to stall is excellent. The reduction in lift curve slope at high $\alpha$ and the gentle nature of the stall indicate that the two both experience trailing edge type stall. Model 5, however, stalls about 2° earlier than model 12, although above this incidence $C_n$ for model 12 is no longer increasing appreciably. Another significant difference between the two tests is the size of the hysteresis loops; for model 12 it is quite wide, with fully attached behaviour starting about 4° lower than the stall incidence, while for the model 5 the corresponding difference is about 1°. Flow visualisation shows that strong corner flows develop at the model/wall junction, and the subsequent downwash distribution along the aerofoil chord is different for the two models. Thus, the differences cited above are likely to be a combination of wake constraint/ downwash effects, which are different for the two aerofoils.

### 3.2 Ramp-up motion

Shown in figures 4a and 4b are comparisons of $C_n$ and $C_m$ data for ramp-up tests on the model 5 and model 12 at R=1.0 and r=0.018.

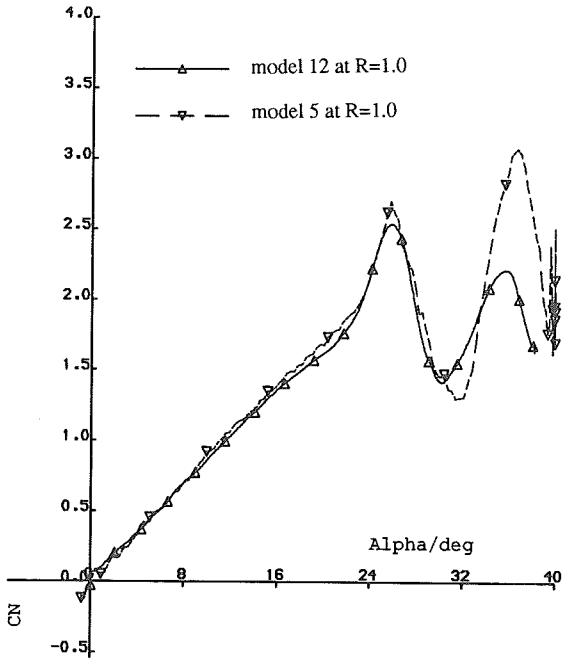


Figure 4a $C_n$ plotted against $\alpha$. Ramp-up tests for model 12 and model 5 at R=1.0 and r=0.018

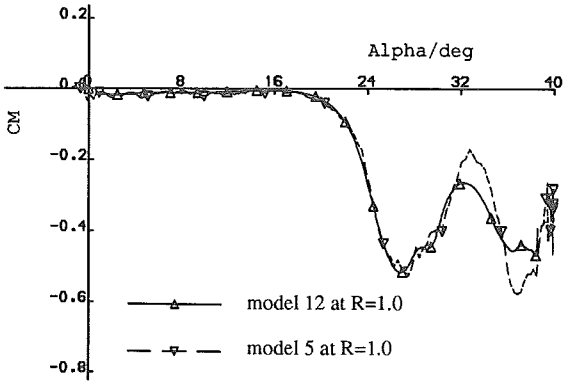


Figure 4b $C_m$ plotted against $\alpha$. Test conditions as for figure 4a

The gross features are the same for the two tests, although there are slight differences in the pitching moment behaviour after the break. However, large differences are apparent in both the $C_n$ and $C_m$ histories after the stall vortex has passed over the trailing edge (i.e. above $\alpha$=26°), which seem to be connected with changes in the wind tunnel dynamic pressure as the model pitches up. Figure 5 shows the time change of DP for the data of figure 4.

Prior to and during dynamic stall, the changes in DP are negligible. After the stall vortex has passed over the trailing edge, model 12 shows a monotonic decrease in DP, while for model 5 there is a significant oscillation.

These DP changes are the result of wake formation. If the oscillations are taken into account, the post-stall differences between model 12 and model 5 in the $C_n$ and $C_m$ behaviour are not so great, although it may be that for the case of model 5 the

phenomena are being driven by the DP changes. It is emphasised, however, that the gross features are the same for the two models.

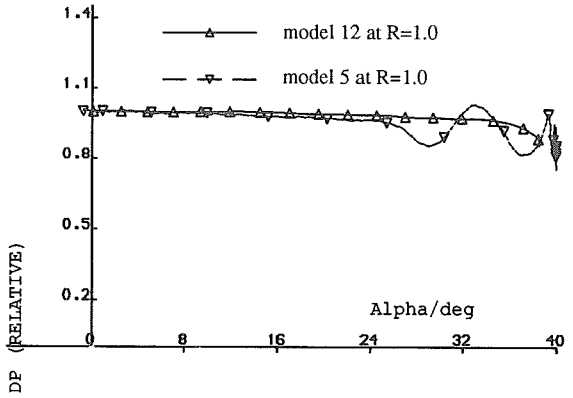


Figure 5 Dynamic pressure plotted against α. Test conditions as for figure 4a

A study of Re effects on model 5 shows that $C_{n\ rise}$ and $C_{n\ max}$ occur earlier, while $C_{n\ max}$ is slightly smaller at R=1.0 compared to that at R=1.5. In addition the $C_n$ curve slope at high α prior to stall is smaller, which may be attributed to increased boundary layer thickening. Figures 6a-c summarise the comparisons between the model 5 at R=1.5 and model 12 at R=1.0 in terms of $C_{n\ max}$, α at $C_{n\ max}$ and α at $C_{n\ rise}$. Included on these figures are the available data for model 5 at R=1.0.

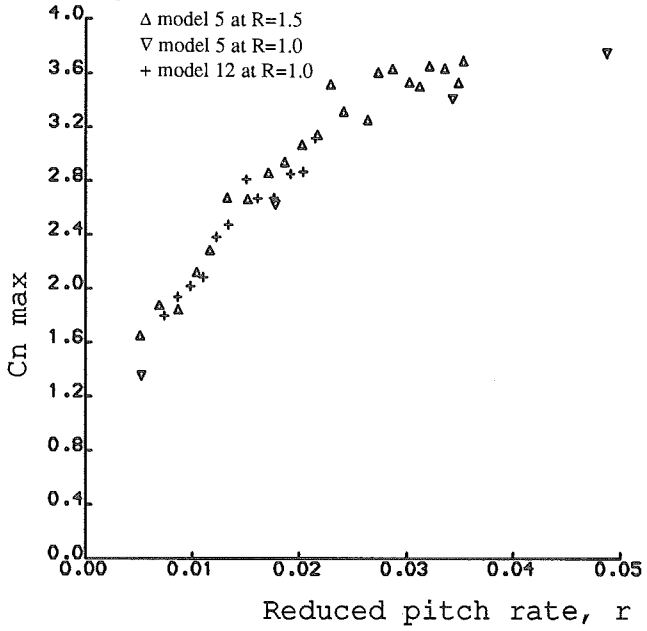


Figure 6a $C_{n\ max}$ plotted against r for ramp-up tests. Model 5 at R=1.5 and R=1.0, model 12 at R=1.0

The $C_{n\ max}$ values for model 12 at R=1.0 and model 5 at R=1.5 are virtually identical, which in view of the above description of the Reynolds number effects on model 5 implies a constraint effect, and may be connected with the fall in DP. The differences between the incidences are consistent with the changes expected with a fall in Re, and the model 5 results at R=1.0 tend to support this view.

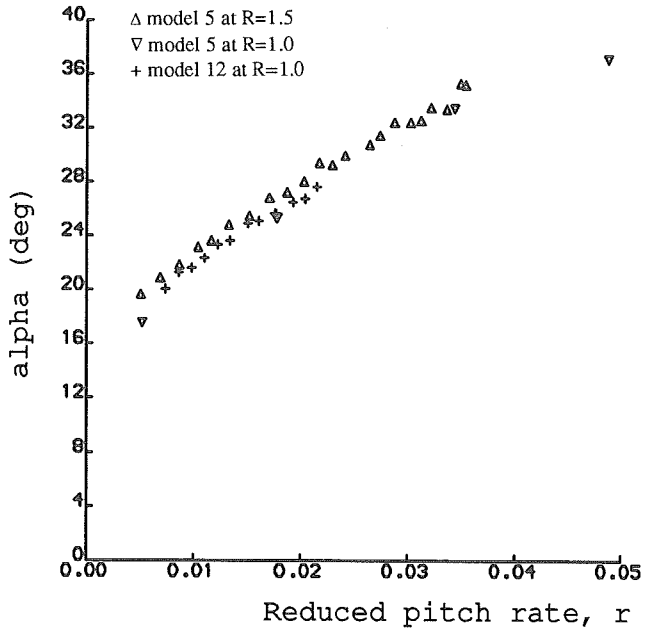


Figure 6b α at $C_{n\ max}$ plotted against r for ramp-up tests. Test conditions as for figure 6a

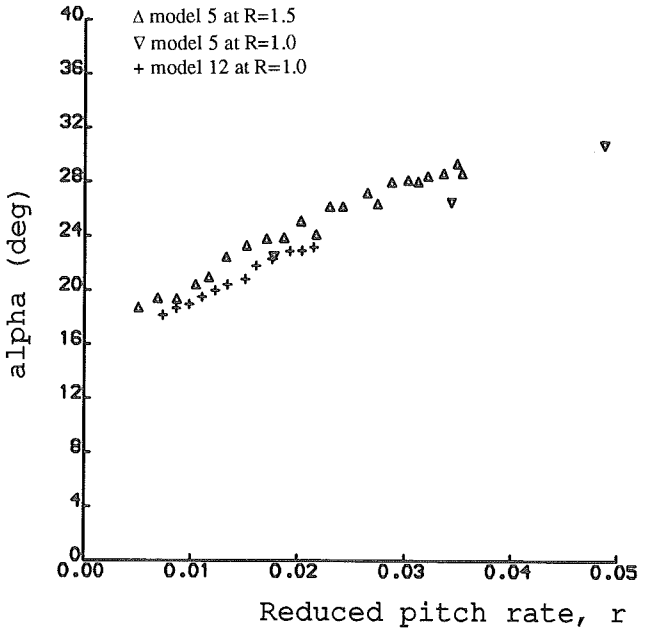


Figure 6c α at $C_{n\ rise}$ plotted against r for ramp-up tests. Test conditions as for figure 6a

The remaining feature to be considered for the ramp-up tests is the stall vortex convection speed. As the stall vortex passes over the aerofoil surface local suction peaks are induced, and the timing of these suction peaks indicates the speed[3]. Shown in figure 7 are the convection speed measurements for model 12 and model 5 as a function of reduced pitch rate.

Note that the model 5 tests are for R=1.5, while the model 12 tests are for R=1.0 and R=0.8. Only a few results are available for the model 12 at such high pitch rates owing to the pitching rate limits of the actuator. The data presented show that the convection speeds are slightly higher for the model 12 than for

the model 5. It may be that this difference is a Reynolds number effect. However, the scatter for the model 5 results is high compared to the mean convection speed, which renders less significant the slightly higher mean speed for the model 12.

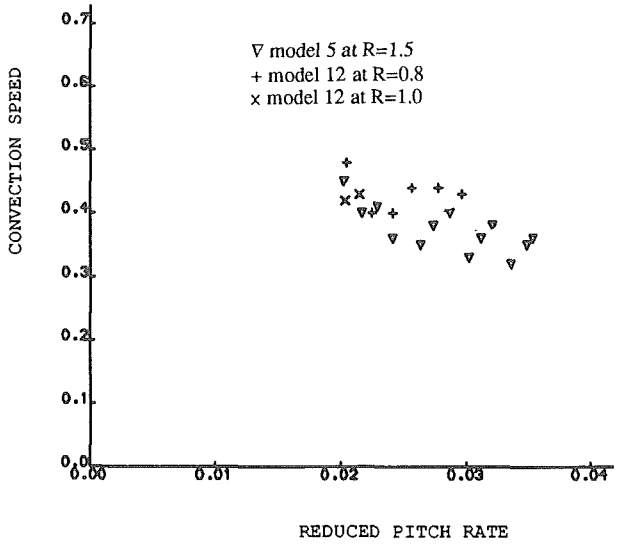


Figure 7 Stall vortex convection speed plotted as a function of reduced pitch rate for the NACA 0015.

The data described above strongly suggest that wind tunnel constraint (within the limits tested) has no first order effects upon the dynamic stall process during ramp-up motions, although there are significant post-stall differences, which appear to be the result of larger DP changes during model 5 testing.

3.2 Ramp-down motion

Reynolds number effects on the model 5 ramp-down test data will first be described. Figure 8 shows a comparison of model 5 $C_n$ data at r=-0.032 for R=1.5 and R=1.0.

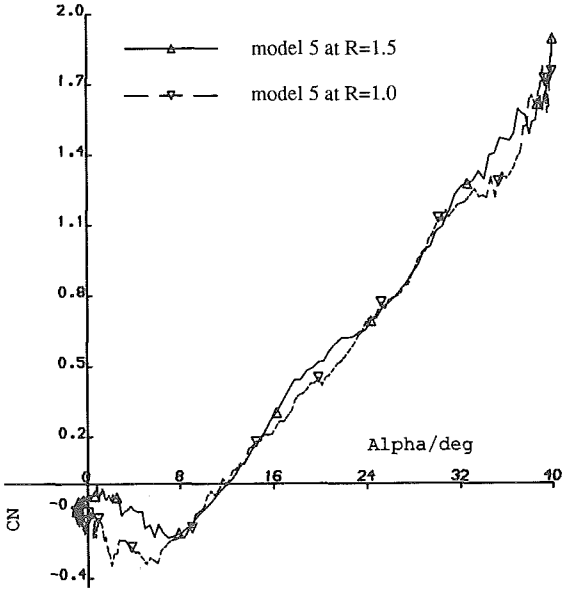


Figure 8 $C_n$ plotted against $\alpha$ for ramp-down motion at r=-0.0317. Model 5 at R=1.5 and R=1.0

The ramp-down test starts from 40° and finishes at -1°. During the initial phase of the motion to about 8°, the responses for the two Reynolds numbers are more or less the same as each other. At $C_n$=0.0 the attachment position is at about x/c=0.1 for the R=1.0 case and x/c=0.14 for the R=1.5 case, which indicates a delay in attachment between the two tests (flow attachment at a given transducer position is measured in terms of a characteristic pressure response described by Niven et al.[5]). $C_{n\,min}$ is related to the attachment position; for R=1.5, it occurs when the attachment position is at about x/c=0.37, while for R=1.0 the corresponding attachment position is over the mid-chord. $C_{n\,min}$ is delayed by 2° for R=1, and as a consequence $C_{n\,min}$ itself is lower at -0.3 compared to -0.2 for R=1.5. The Reynolds number trends described above are also found at r=-0.005 and r=-0.017 (note in these cases that the pitch rate is insufficient to induce negative $C_n$). A decrease in Reynolds number delays the onset of attachment, which seems reasonable, although at the lower Reynolds number $C_{n\,min}$ is additionally delayed until attachment is further along the aerofoil surface. The reason for this is unclear and is the subject of further work.

A comparison of model 12 and model 5 results shows that the overall features of the aerodynamic coefficient responses and attachment behaviour are preserved. Some significant differences emerge, however. Both models were ramped down from 40°, although the stopping incidences for the model 5 and model 12 tests were -1° and -9° respectively. $C_n$ data for model 12 and model 5 are shown in figure 9 for R=1.0 and r=-0.032.

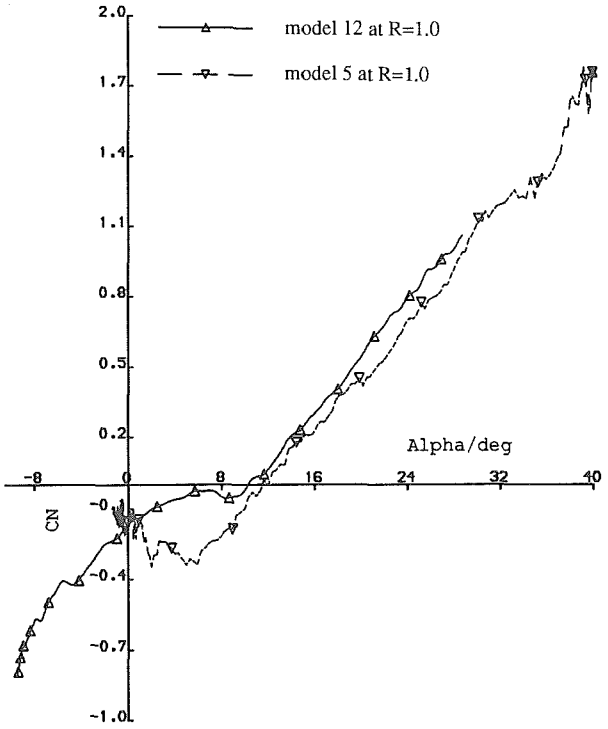


Figure 9 $C_n$ plotted against $\alpha$ for ramp-down motion at r=-0.031. Model 12 and model 5 at R=1.0

The first point to note (although it is not too obvious) is that the gradient of the separated $C_n$ curve for model 12 is lower than that of model 5. This is observed at all pitch rates. Figure 10 shows the gradients for the two models plotted as a function of reduced pitch rate.

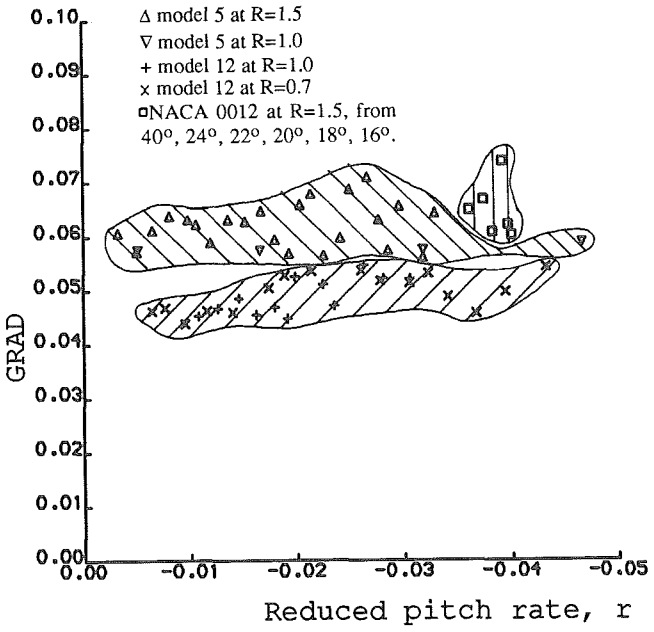


Figure 10 Gradient of fully separated portion of $C_n$-$\alpha$ curve during ramp-down motion plotted as a function of reduced pitch rate. Results are shown for model 5 at R=1.5 and R1.0, model 12 at R=1.0 and R=0.7 and NACA 0012 tests from differing start incidences at R=1.5

At higher r, the model 12 gradients appear to be tending towards the model 5 values. It was suspected that the difference in gradients may be a result of DP changes during the ramp-down motion. Dynamic pressure increases during the ramp-down motion since the blockage drops, and the increase is larger for model 5 than for model 12, which could help explain the difference in the separated $C_n$ curve gradient (note that the gradients are different even when the DP changes are accounted for). However, ramp-down tests from differing incidences on a NACA 0012 of the same chord length as model 5 show that the separated $C_n$ curve slope is the same within the expected level of scatter for each start incidence, even though the DP response is different for each case (these results are also shown on figure 10). When the $C_n$ curve slopes for the upper and lower surfaces are compared, it is found that the differences are the same for each surface; model 5 gradients are higher by 25%, which is not a Reynolds number effect.

Secondly there is a significant difference in the value of $C_{n\,min}$ and the incidence at which it occurs. Figure 9 shows that for model 5 $C_{n\,min}$ has a value of -0.375 and occurs at $\alpha$=5.6°, while for model 12 the respective figures are -0.05 and 8.7°. Consequently the chordwise positions of attachment at $C_{n\,min}$ are quite different, with x/c=0.4 for model 12 and x/c=0.5 for model 5.

To summarise the above, a comparison of model 12 and model 5 data shows different $C_n$ curve slopes prior to $C_{n\,min}$, and a smaller magnitude and earlier occurrence of $C_{n\,min}$ for model 12. In addition, attachment is delayed by some 2° for the model 5, which does not account for the phase difference in $C_{n\,min}$.

## 4. Discussion

The above comparisons have shown that the gross features of the responses to ramp-up and ramp-down motion are the same for the two models. For ramp-up motion, the difference in wind tunnel constraint has a negligible effect prior to and during stall. There is evidence, however, that dynamic pressure oscillations for the model 5 affect the post-stall response. In the case of ramp-down motion, constraint effects are apparent throughout the whole duration of the test. The separated flow lift curve slopes are different for the model 12 and model 5, and the attachment itself is affected, with model 5 being delayed with respect to model 12 by some 2° at r=-0.03. $C_{n\,min}$ is also lower for the model 5 and occurs when the attachment position is further along the chord.

During ramp-up motion, the wake needs time to develop. It is well known that oscillating a bluff body transversely to the free stream can synchronise vortex shedding over the span of the model (Koopman [8]). It could therefore be expected that the development of three-dimensional wake structures be suppressed during ramp-up motion.

In the case of ramp-down tests, however, the wake is almost certainly three- dimensional prior to the onset of motion, and the degree of three-dimensionality is different for the model 12 and the model 5. It seems unlikely that the effects of two-dimensional wake constraint on the model 5 are significant, since the ramp-down tests for the NACA 0012 from successively lower incidences hardly differ from one another in terms of $C_n$-$\alpha$ gradient, $C_{n\,min}$ and $\alpha$ at $C_{n\,min}$. The approximately 1.5° phase shift between model 12 and model 5 on the separated flow portion of the $C_n$-$\alpha$ curve shown in figure 9 suggests that the two models experience different levels of downwash during ramp-down tests. The phase differences are not constant since the $C_n$-$\alpha$ gradients for the two models are not the same as each other, and this suggests that the amounts of downwash for the two models differ with incidence. From figure 9 either model 12 appears to suffer increased upwash *or* model 5 suffers downwash. Niven & Galbraith [6] found that there is a downwash distribution over the span of the large chord models, so the increased upwash experienced by model 12 may be interpreted as *less* downwash. In the context of Niven & Galbraiths'[6] observations, this represents a decreased constraint effect.

A NACA 23012C model of the same chord length as model 5 was tested during ramp-down motion with fins equidistant from the centre span [6]. The effect of the fins was to isolate the corner flows and to reduce the aspect ratio from 2.92 to 1.6. Attachment was found to occur earlier during a steady test. For ramp-down tests the separated flow $C_n$ curve slope remained unaltered, although $C_{n\ min}$ occurred earlier by 1.5° for the reduced AR case. It seems that the presence of the fins cannot have appreciably altered the structure of the three dimensional flow over the NACA 23012C; the *reduction* in AR has caused earlier attachment, while when model 12 and model 5 are compared, the *increase* in AR results in earlier attachment and a significant difference in the separated $C_n$ curve slope. Thus it seems likely that the model 12 tests involve quite different three dimensional flow patterns.

No explanation is offered at present for the differing lift curve slopes between model 12 and model 5, other than that the three dimensional stall pattern is altered (typical three dimensional patterns are described by Moss and Murdin [8]). The ramp-down behaviour will be influenced by the dynamic behaviour of the three-dimensional stall cells, and little is known about this. In spite of the apparently different downwash model 5 attachment is *delayed* with respect to model 12 by some 1.5° over the aft 95% of chord. Thus the lower $C_{n\ min}$ for the model 5 tests is a combination of the delayed attachment, the higher gradient of the separated flow lift curve slope and the minimum lift occurring when attachment is further along the aerofoil chord.

It has been postulated that the mechanism of attachment involves the damping of turbulent structures from length scales associated with a turbulent separated shear layer to those of an attached boundary layer[5]. Attachment rates and time delays between attachment at the leading edge and the trailing edge are not significantly affected by the difference in wind tunnel constraint, even though model 5 attachment is delayed with respect to model 12. An interesting point to note is that a model 12 test at R=1.0 more closely resembles a model 5 test at R=1.5 than one at R=1.0 in terms of incidence at $C_{n\ min}$ (compare figures 8 and 9) and attachment history (see figure 11). Therefore constraint effects may have affected the damping mechanism, the length scales of the turbulent structures or the turbulent energy spectrum.

Although constraint does not appear to have significantly influenced dynamic stall during ramp-up tests, the post-stall behaviour and attachment during ramp-down are affected, and therefore during an oscillatory test involving full separation and re-attachment it is likely that constraint effects will be observed. Coupled with this there is the possibility that unsteady aerodynamics experiments could be wind tunnel dependent, in that dynamic pressure changes (which force the post-stall behaviour) depend upon the blockage and the wind tunnel motor power.

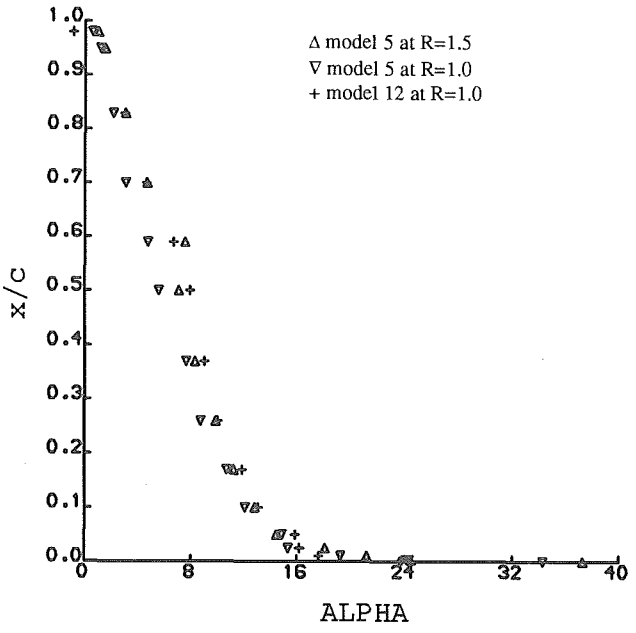


Figure 11 Re-attachment loci for ramp-down motion at r=-.031. Model 5 at R=1.5 and R=1.0 and model 12 at R=1.0

## 5. Conclusions

Two NACA 0015 models of different blockage and aspect ratio were tested using the same facility.

The lift and pitching moment responses of the two models during ramp-up motion were found to be negligibly small prior to and during dynamic stall, although after stall differences were observed which may be attributed to dynamic pressure changes during testing. Stall vortex convection speed was seen to be independent of reduced pitch rate for both models, and to agree within the level of scatter. It is therefore concluded that ramp-up experiments are insensitive, to a first order, to wind tunnel constraint within the ranges tested.

The gross features of the response during ramp-down motion were the same for the two models, although a delay in attachment and higher separated flow lift curve slope were observed with the model of higher constraint and lower aspect ratio. In addition, the attachment time delay and attachment rates were not seen to significantly vary between the two models.


## Acknowledgements

The work was carried out with the financial assistance of the Science and Engineering Research Council. In addition, the contribution of the technical staff of the Department of Aerospace Engineering, The University of Glasgow is greatly appreciated.

## References


1. McCroskey, W.J., Carr, L.W. & McAlister, K.W. 'Dynamic Stall Experiments on Oscillating Aerofoils' **AIAA Journal 14,** p57 (1976)

2. Green, R.B., Galbraith, R.A.McD. & Niven, A.J. 'Measurements of the Dynamic Stall Vortex Convecyion Speed' Presented at the 17th European Rotorcraft Forum, Berlin, Greater Germany, September 1991.

3. Lorber, P.F. & Carta, F.O. 'Unsteady Stall Penetration Experiments at High Reynolds Number' **AFOSR** TR-87-1202, **UTRC** R87-956939-3 (1987)

4. Green, R.B., Galbraith, R.A.McD. & Niven, A.J. 'The Convection Speed of the Dynamic Stall Vortex' **AFOSR**-89-0397 A, University of Glasgow Aero Rept. 9202.

5. Niven, A.J., Galbraith, R.A.McD. & Herring, D.G.F. 'Analysis of Reattachment During Ramp Down Tests' **Vertica, 13,** p187 (1989)

6. Niven, A.J. & Galbraith, R.A.McD. 'Experiments on the Establishment of Fully Attached Flow from the Fully Stalled Condition During Ramp-Down Motions' Presented at 17th ICAS Congress, Stockholm, Sweden, 1990

7. Koopman, G.H. 'The Vortex Wakes of Vibrating Cylinders at Low Reynolds Numbers' **J. Fluid Mech. 28,** p501 (1967)

8. Moss, G.F. & Murdin, P.M. 'Two-Dimensional Low-Speed Tunnel Tests on the NACA 0012 Section Including Measurements Made During Pitch Oscillations at the Stall' **A.R.C. C.P 1145** (1971)